

Fluctuation-Dissipation Relations for Motions of Center of Mass in Driven Granular Fluids under Gravity

Jun'ichi Wakou^{1,2*} and Masaharu Isobe^{3†}

¹*Miyakonojo National College of Technology, Miyakonojo-shi, Miyazaki, 885-8567, Japan*

²*Department of Physics, Kyushu University 33, Fukuoka 812-8581, Japan*

³*Graduate School of Engineering, Nagoya Institute of Technology, 466-8555, Japan*

(Dated: March 22, 2019)

We investigate a validity of fluctuation-dissipation relations in a nonequilibrium stationary state of fluidized granular media under gravity. A phenomenological Langevin-type theory describing the fluctuation of center of mass height, which was originally constructed for one-dimensional granular gas on a vibrating bottom plate, is generalized to any dimensions even for the case that the vibrating bottom plate is replaced by a thermal wall. The theory gives analytical expressions for the power spectrum and response function of the center of mass height; furthermore, it predicts a fluctuation-dissipation relation between them, which is known to be satisfied at equilibrium, with a modification that equilibrium temperature is replaced by an effective temperature defined by a kinetic energy of the center of mass. To check these explicit theoretical predictions, we performed extensive and accurate event-driven molecular dynamics simulations for the model system with a thermal wall at the bottom. We found that the power spectrum and response function of the center of mass height show good agreement with theoretical predictions within a range of time scales in which our theory is valid. As the most remarkable result, it is shown that a fluctuation-dissipation relation for the granular system is well satisfied especially at a large frequency (short time) region in a wide range of system parameter. We finally remark that the relation between systematic deviations at a small frequency (long time) region and time scales of the driven granular system.

PACS numbers: 45.70.-n, 47.70.Nd, 05.40.-a, 05.70.Ln

I. INTRODUCTION

Granular materials show fluid like behavior when they are supplied sufficient energy by external vibration. Such fluidized states of granular matter have been studied as an interesting example of nonequilibrium fluids that exhibits a rich variety of phenomena such as convection, pattern formation on the surface, and segregation (see Ref. [1] and references therein). Besides these pattern forming instabilities, a plain stationary state of vibrated granular fluids without any complex spatial structures serves as an archetypal example of nonequilibrium stationary states (NESSs). It has been a fundamental subject for long years to find any thermodynamic-like description or to identify common property of fluctuations in a wide variety of NESS in nature.

One of important issues, addressed in this paper, is to clarify the validity of a fluctuation-dissipation relation (FDR) in granular fluids subject to external vibration. A FDR connects the response of an equilibrium system to a small perturbation with the time correlation of spontaneous fluctuations in the system without perturbation. It has attracted recently a lot of interest how a FDR is violated or should be modified in ageing systems such as glass and in NESSs of various systems. (See Refs. [2, 3] as recent reviews.)

For granular systems, FDRs have been studied for sev-

eral situations. Many works have devoted to the case of freely cooling granular gas, in which the gas develops freely without external forces and “cools” down as a result of dissipative nature of the grain interactions, aiming to derive a (modified) Green-Kubo relation and to calculate transport coefficients using it [4–7]. While there is no stationary state of freely cooling granular gas, a NESS of granular gas can be achieved by supplying energy from outside by means of external driving. A typical experimental mean of injecting energy is shaking a container or vibrating a bottom wall (see, e.g., Ref. [8]). In the case that the shaking (or vibrating) is strong enough to inject energy to all grains by frequent collisions with the vibrating wall, the effect of the vibrating wall is often modeled using a thermal bath that couples to every particle. FDRs in such uniformly driven granular systems have been studied in Refs. [9–13]. Puglisi et al. [9] carried out numerical simulations of a model of uniformly driven granular gas and studied FDRs for two different observables. They observed the FDRs are well satisfied if the equilibrium temperature in the FDR for a system at equilibrium is replaced by the granular temperature defined as the mean-square fluctuation of the grain velocity. Garzó [10] studied analytically diffusion of impurities immersed in a granular gas under influence of uniform driving forces and showed that a modified form of the Einstein relation, in which the temperature of the gas is replaced by the temperature of the impurity, is violated due to the non-Maxwellian behavior of the impurity velocity distribution function. Bunin et al. [12] analyzed a mean-field model of uniformly driven granular gas and showed that an effective temperature defined by a FDR

*Electronic address: wakou@cc.miyakonojo-nct.ac.jp

†Electronic address: isobe@nitech.ac.jp

depends on frequency. In the case that the shaking (or vibrating) is not strong enough to be regarded as uniform driving, energy injection through a boundary has to be explicitly considered. Brey et al. [13] studied numerically the fluctuations of volume of a vibrated low density granular gas confined by a mobile piston on the top. In this system energy is supplied from the vibrating bottom wall. They discussed interpretation of an effective temperature defined by requiring the same relation between fluctuations of volume and compressibility as in equilibrium systems. FDRs and effective temperatures in much denser systems have also been studied by several authors [14-17]. Among these studies, we refer to an experimental study by D'Anna et al. [17], since their theory based on a Langevin equation formally has the same form as ours although their experimental setup is very different from ours. They carried out an experiment observing fluctuating motion of a torsion oscillator immersed in vibration-fluidized granular matter and found that it can be described as a first approximation by a formalism on Brownian motion in the equilibrium and a FDR with an effective temperature approximately holds.

This paper is intended to investigate fluctuating motion of the center of mass (COM) in a NESS of a granular matter fluidized by an external energy source located at a bottom wall, under influence of gravity. Instead of using macroscopic probes such as a piston [13] and a torsion oscillator [17], we focused on position of the COM that is observable by means of digital high speed photography in experiments [18]. Our major motivation to study fluctuations of the COM is that a simple (or universal) law might hold as a result of the following properties: First, the fluctuations of macrovariables like position of the COM often possess the largest time scale in the system. Secondly, they are expected to have a Gaussian property in a similar sense as the central limit theorem. (In the case of a Markovian stochastic process, a Gaussian property of fluctuations of macrovariables can indeed be derived from a master equation of the Markovian process [19].) With this expectation, we proposed a phenomenological theory based on a simple formalism on Brownian motion that describes motion of the COM height in a NESS of a one-dimensional vibrated granular fluid [20]; we found that the important qualitative features of dynamics of the COM in event-driven molecular dynamics (MD) simulations are all accounted for by the theory. The theory was extended to a two-dimensional granular fluid on a thermal wall [21]. In this paper we will show that when we apply the phenomenological theory to granular fluids in higher dimensions, careful consideration of time scales in granular hydrodynamics [22, 23] is necessary. Within a time range in which our theory is valid, it predicts an existence of a FDR except that the equilibrium temperature in the FDR for an equilibrium system must be modified by an effective temperature of velocity fluctuation of the COM. In order to test our prediction, we performed extensive and accurate event-driven MD simulations for a two-dimensional system of inelastic hard

disks on a thermal wall.

Our main result is that a FDR with an effective temperature holds within statistical uncertainty in simulations in a large frequency (short time) region while it is violated in a small frequency (long time) region. The effective temperature is defined by a kinetic energy of the COM. We observed in our simulations that the ratio between the effective temperature and the global granular temperature increases with inelasticity; the former can be more than 4 times larger than the latter for the highest inelasticity case.

This paper is organized as follows. In Sec. II, we describe a model granular system and discuss important time scales in the system. In Sec. III, the Langevin equation is introduced, and analytical expressions for power spectrum and response function of the COM height are expressed briefly. We also remark on the FDR between these two functions. Note that a complete derivation of the Langevin equation and detail calculation for the power spectrum and the response function are summarized in Appendix A and B, respectively. As the numerical tests, the comparison between the theoretical predictions and extensive event-driven MD are shown in Sec. IV. Finally, in Sec. V, we summarize the main results of a validity of FDR in this paper and remark on the relation between systematic deviations at a small frequency (long time) region and time scales of the driven granular system.

II. THE MODEL SYSTEM

A. System

As a model of grains bouncing on a vibrating bottom plate under gravity, we consider a d -dimensional system of N inelastic particles on a “thermal” bottom wall in a constant gravitational field g . The particles in the system have diameter σ and mass m ; the total mass of particles is denoted by M ($= Nm$). The thermal wall is kept at a constant temperature T_0 , which plays a role of a heat source supplying sufficient translational energy to the particles to fluidize them. The z -direction is chosen to be opposite to the direction of gravity, and the thermal wall is fixed at $z = 0$. For simplicity, we adopt periodic boundary conditions in horizontal directions in order to ignore the boundary (side-wall) effects. Collisions between particles are inelastic; inelasticity of the particle collisions is characterized by a normal restitution coefficient r . In order to avoid any pattern forming instability along horizontal directions, we choose both the inelasticity and linear scales of the system in horizontal directions are sufficiently small so that the system remains homogeneous in horizontal directions. These conditions of setting will be discussed in more detail in Sec. IV.

B. Time scales

Before discussing on important time scales in the system, let us define several quantities that characterize macroscopic property of the system. We first define the kinetic energy per particle as $K(t) \equiv (1/N) \sum_{i=1}^N m v_i(t)^2 / 2$, the long time average of $K(t)$ in a NESS as $\overline{K} \equiv \lim_{T \rightarrow \infty} (1/T) \int_0^T K(t) dt$ (hereafter the overline on a quantity represents the long time average of the quantity in a NESS), the global granular temperature T by $k_B T \equiv (2/d) \overline{K}$, where k_B is the Boltzmann constant, and the thermal velocity as $c \equiv (dk_B T / m)^{1/2} = (2\overline{K}/m)^{1/2}$. A characteristic length scale of the system in vertical direction l is then defined as $l \equiv c^2/g$.

Bromberg et al. [23] have suggested that there are three important time scales in this system at a level of hydrodynamics: macroscopic oscillation time τ_{osc} (referred to as “fast time scale” in Ref. [23]), relaxation time for thermal conduction τ_{therm} , and relaxation time for collisional dissipation τ_{diss} .

For the sake of simplicity in estimation of these time scales, let us assume here the system is nearly homogeneous although this is not true for small r and large N . The time scale τ_{osc} represents a period of the slowest oscillation in vertical direction, that is, a period of sound mode with the longest wavelength. Thus $\tau_{osc} \sim l/c_s$, where c_s is a sound velocity. Assuming $c_s \sim c$ which is well satisfied in the case of normal gas, τ_{osc} can be estimated as $\tau_{osc} \sim c/g$. Since l/c_s also characterize the relaxation time of pressure, τ_p , we can regard τ_p and τ_{osc} are on the same order: $\tau_p \sim \tau_{osc} \sim c/g$. The relaxation time for thermal conduction τ_{therm} is estimated as $\tau_{therm} \sim l^2/(\kappa/\rho c_p)$, where κ is the thermal conductivity, ρ is the mass density, and c_p is the specific heat at constant pressure [24]. ρ can be estimated as $\rho \sim M/(lA) \sim mN_z/(l\sigma^{d-1})$, where A represents the area of the bottom plate in the case of three dimensions (A represents the length of the bottom plate in two dimensions and $A = 1$ in one dimension) and N_z represents the number of monolayers at rest. κ and c_p are obtained from kinetic theory for elastic spheres and disks [25]: $\kappa \sim k_B c/\sigma^{d-1}$ and $c_p \sim k_B/m$. Substituting these results, we obtain $\tau_{therm} \sim N_z c/g$. The relaxation time for collisional dissipation τ_{diss} can be estimated as the inverse of $(1-r^2)\nu$, where ν is the collision frequency between two particles. Substituting the lowest order estimation of ν based on kinetic theory, $\nu \sim \rho\sigma^{d-1}c/m \sim N_z c/l$, we obtain $\tau_{diss} \sim (1-r^2)^{-1}c/(N_z g)$.

The time scales estimated above are summarized as follows:

$$\begin{aligned} \tau_{osc} &\sim \tau_p \sim \frac{c}{g}, & \tau_{therm} &\sim N_z \frac{c}{g}, \\ \tau_{diss} &\sim [N_z(1-r^2)]^{-1} \frac{c}{g}. \end{aligned} \quad (1)$$

It is important to note that the all time scales, τ_{osc} , τ_p , τ_{therm} , and τ_{diss} are proportional to c/g . This means

that for a system with given N_z and r , macroscopic dynamics with time that is scaled by c/g are independent of g . We will utilize this fact later in order to obtain a frequency response function in an efficient way.

There are three dimensionless parameters obtained from these three time scales. The first is $\tau_{therm}/\tau_{osc} \sim N_z$. The second is $\tau_{osc}/\tau_{diss} \sim N_z(1-r^2)$. The third is $\tau_{therm}/\tau_{diss} \sim N_z^2(1-r^2)$. The first and third parameters are governing parameters of hydrodynamic description of the system introduced by Bromberg et al. [23]. They have shown that steady state profile is governed only by a parameter

$$\Lambda \equiv \frac{\sqrt{\pi}}{2} N_z(1-r^2)^{1/2}, \quad (2)$$

which is proportional to $(\tau_{therm}/\tau_{diss})^{1/2}$. If $r \ll 1$, the second parameter τ_{osc}/τ_{diss} is related to $X \equiv N_z(1-r)$ that plays a role of a governing parameter of transition from a condensed phase into a fluidized phase in a system of one-dimensional column of beads on vibrating bottom plate [26]. In our study, we consider the case $N_z \gg 1$ and assume $\tau_{therm} \gg \tau_{osc}$ in the following theoretical analysis.

III. THEORETICAL DERIVATIONS OF FLUCTUATION-DISSIPATION RELATION

In this section, we summarize the theoretical derivation of (i) the power spectrum, (ii) frequency response function, and (iii) FDR between (i) and (ii). Firstly, we introduce a Langevin equation as a first approximation which describes fluctuating motion of the COM within the fast time scale of τ_{osc} and τ_p . Note that the derivation of our theory has already been published in Ref. [20]. We assume $\tau_{therm} \gg \tau_{osc}$ as mentioned above, and focus on dynamics of the COM in the time scale of τ_{osc} ignoring a significant slow relaxation process of fluctuations of global granular temperature around its stationary value $(2/d)\overline{K}/k_B$. The effect of this slow dynamics of granular temperature and validity of our assumption of time scale will be discussed later.

We summarize details of derivation of our Langevin formalism in Appendix A and show here the final result. Let us denote the height of the COM of granular fluids at time t as $Z(t)$, a time average of $Z(t)$ over a long time interval in a NESS as \overline{Z} , and small deviation of $Z(t)$ from \overline{Z} as $\delta Z(t) \equiv Z(t) - \overline{Z}$. A Langevin equation for fluctuating motion of $\delta Z(t)$ is given by (see Eq. (A5) in Appendix A),

$$\frac{d^2 \delta Z}{dt^2} = -\Omega^2 \delta Z - \mu \frac{d\delta Z}{dt} + \frac{R(t)}{M}, \quad (3)$$

where $R(t)$ represents a random force which is assumed to be a Gaussian white noise:

$$\langle R(t) \rangle = 0, \quad \langle R(t)R(t') \rangle = I\delta(t-t'). \quad (4)$$

The brackets $\langle \dots \rangle$ denote an average over the random force. In NESS, it is reasonable to assume $\langle Z(t) \rangle_{st} = \bar{Z}$, where $\langle \dots \rangle_{st}$ represents the average in a stationary state. The constant I represents intensity of the random force, which is related to the second moment of the velocity fluctuations of the COM. This relation can be obtained by calculating the average kinetic energy of the COM motion in z -direction per particle: $K_{CMz} \equiv \langle MV_z(t)^2/2 \rangle_{st}$, here V_z is the z -component of the velocity of the COM: $V_z(t) \equiv \frac{dZ(t)}{dt}$. Using an analytical solution Eq. (B1) of the Langevin equation, we obtain $K_{CMz} = I/4M\mu$. Hence, the constant I is identified as follows:

$$I \equiv 4M\mu K_{CMz}. \quad (5)$$

This is indeed the same procedure to determine the noise intensity I when the Langevin equation describes fluctuations in equilibrium at temperature T . In equilibrium, equipartition of energy implies $K_{CMz} = k_B T/2$. Thus, we obtain the well-known result $I = 2M\mu k_B T$. In the case of NESS of granular fluids, violation of equipartition of energy is observed in various systems (see Ref. [27] and references therein). We will show later a result of numerical simulations that clearly shows violation of equipartition, $K_{CMz} \neq k_B T/2$, when we recognize T as the global granular temperature.

The coefficients Ω and μ describe an angular frequency of the slowest oscillation of the COM height and frictional coefficient with respect to relative motion of the COM height against the bottom wall, respectively. According to the time scales we consider here, we assume $\Omega \sim \tau_{osc}^{-1}$ and $\mu \sim \tau_p^{-1}$, and write them as,

$$\Omega = \hat{\Omega}g/c, \quad \mu = \hat{\mu}g/c. \quad (6)$$

Since values of the coefficients $\hat{\Omega}$ and $\hat{\mu}$ cannot be estimated in our phenomenological theory, they are fixed as fitting parameters when we compare results of simulations with the theoretical predictions.

Power Spectrum: The power spectrum $S(\omega)$ that represents property of fluctuations of Z around NESS is defined as the Fourier transform of the time correlation function,

$$S(\omega) \equiv \int_{-\infty}^{\infty} dt e^{-i\omega t} \langle \delta Z(0) \delta Z(t) \rangle_{st}. \quad (7)$$

Derivation of $S(\omega)$ using the analytic solution of the Langevin equation is straightforward. We express here the final expressions of $S(\omega)$ in this system (See Appendix B for more detail deviation),

$$S(\omega) = \frac{1}{M} \frac{4\mu K_{CMz}}{(\Omega^2 - \omega^2)^2 + (\mu\omega)^2}. \quad (8)$$

Response Function: The frequency response function $\chi(\omega)$ which characterizes linear response of Z in NESS against a small external force $\varepsilon f(t)$ can be defined as,

$$\chi(\omega) \equiv \lim_{\varepsilon \rightarrow 0} \langle \delta \tilde{Z}(\omega) \rangle / \varepsilon \tilde{f}(\omega), \quad (9)$$

where $\delta \tilde{Z}(\omega)$ and $\tilde{f}(\omega)$ are the Fourier transform of $\delta Z(t)$ and $f(t)$, respectively. The analytical expression of $\chi(\omega)$ is given by (See Appendix B for derivation),

$$\chi(\omega) = \frac{1}{M} \frac{1}{\Omega^2 - \omega^2 + i\mu\omega}. \quad (10)$$

According to conventional definition, $\chi(\omega)$ can be decomposed into real $\chi'(\omega)$ and imaginary $\chi''(\omega)$ parts as $\chi(\omega) = \chi'(\omega) - i\chi''(\omega)$. Thus we obtain the following expressions,

$$\chi'(\omega) = \frac{1}{M} \frac{\Omega^2 - \omega^2}{(\Omega^2 - \omega^2)^2 + (\mu\omega)^2}, \quad (11)$$

$$\chi''(\omega) = \frac{1}{M} \frac{\mu\omega}{(\Omega^2 - \omega^2)^2 + (\mu\omega)^2}. \quad (12)$$

Fluctuation Dissipation Relation: Comparing Eqs. (8) and (12), we obtain a following FDR,

$$\frac{\omega S(\omega)}{2k_B T_{eff}} = \chi''(\omega), \quad (13)$$

where T_{eff} is an effective temperature defined as $T_{eff} \equiv 2K_{CMz}/k_B$. This has the same form as the FDR in an equilibrium system except for T_{eff} which replaces the equilibrium temperature.

IV. NUMERICAL SIMULATIONS

In this section, we compare our three theoretical predictions described in the previous section with results of numerical simulation of a two-dimensional granular gas system, which are the power spectrum Eq. (8), the frequency response function Eq. (10), and the fluctuation-dissipation relation Eq. (13). The numerical setting of our system consists of N inelastic hard disks of mass m and diameter σ moving in two-dimensional system on a thermal wall with a fixed temperature T_0 . Here, x - and z -axes are set at horizontal and vertical directions of the system, respectively. The system width is denoted as L and periodic boundary conditions are adopted in the horizontal direction at $x = 0$ and $x = L$. The bottom wall is located at $z = 0$ and there is no top wall. Gravitational force exerts on each disk along negative z -direction. Inelastic collisions between hard disks are considered by normal restitution coefficient r . When a disk collides with a thermal wall at the bottom, it comes off with a value of z -component of velocity v_z sampled from the probability density

$$p(v_z) = \frac{mv_z}{k_B T_0} \exp\left(-\frac{mv_z^2}{2k_B T_0}\right). \quad (14)$$

The horizontal component of velocity does not change during the collision with the thermal wall.

Numerical simulations were performed with an event-driven algorithm devised to enhance speed of calculation in particular in dense hard sphere systems [28]. In the following, all simulation data is presented with mass, length and time in units m , σ , and $\sigma/(k_B T_0/m)^{1/2}$, respectively. This corresponds to choosing $k_B T_0 = 1$. We set $N = 5000$ and $L = 100$, and keep these parameters unchanged throughout this paper. For our main results, $r = 0.99 \sim 0.999$ and $g = 10^{-3}$ are used unless otherwise mentioned. These correspond to $N_z = 50$, $0.05 \leq X \leq 0.5$, and $1.98 \leq \Lambda < 6.25$. A system with the width $L = 100$ and $r \geq 0.99$ is small enough to prevent any horizontal pattern structures (such as ripple and undulation). The global temperature T and the thermal velocity c are calculated using the following formula: $T = \bar{K}/k_B$ and $c = (2\bar{K}/m)^{1/2}$, where \bar{K} is the long time average of the kinetic energy per disk.

A. Macroscopic properties in NESS

In Fig. 1 (top), we show typical snapshots of particle configuration in the system of $N = 5000$ and $g = 10^{-3}$ for $r = 0.999$ and 0.992 . The corresponding area-fraction profiles are plotted in Fig. 1 (bottom). For a nearly elastic case ($r = 0.999$), the profile has one peak around the height $z \simeq 350$, however, the area fraction is relatively dilute less than 0.06 even at the height of the peak. Many inelastic particles are raised up relatively high like the equilibrium profile of the Boltzmann distribution. Contrastingly, in case of $r = 0.992$, the profile drastically changes. The most of particles condense at relatively low height like a cluster; the area-fraction profile show a clear peak upon the low density region around the thermal wall. This state is known as *density inversion state* which has been observed in many experiments [29, 30] and simulations [31, 32] of vibrofluidized granular matter.

In accordance with the theoretical study by Bromberg et al. [23] showing that the steady state is characterized by a single parameter Λ defined in Eq. (2), we plotted in Fig. 2 the average kinetic energy per disk \bar{K} and the average kinetic energy of the COM \bar{K}_{CMz} as a function of Λ . The statistical error bars with the standard deviation were also plotted in all figures throughout the paper. $\Lambda = 0$ (i.e., $r = 1$) corresponds to the equilibrium state where equipartition of energy $2\bar{K}_{CMz} = \bar{K} = k_B T_0 = 1$ is satisfied. The factor 2 comes from the fact that \bar{K}_{CMz} is defined using only z -component of COM velocity. Note that the horizontal component of velocity of the COM vanishes in our simulations because horizontal component of velocity of disks are unchanged at collisions with the bottom wall. While \bar{K} systematically decreases as a power law $\sim \Lambda^{-1.48}$, \bar{K}_{CMz} shows a minimum at $\Lambda \simeq 2$ ($r = 0.999$) and increases with Λ for $\Lambda > 2$. Fig. 2 clearly indicates that equipartition of energy breaks down when $\Lambda > 2$ (i.e., $2\bar{K}_{CMz} \neq \bar{K}$). Similar behavior in much smaller systems has been preliminarily reported by

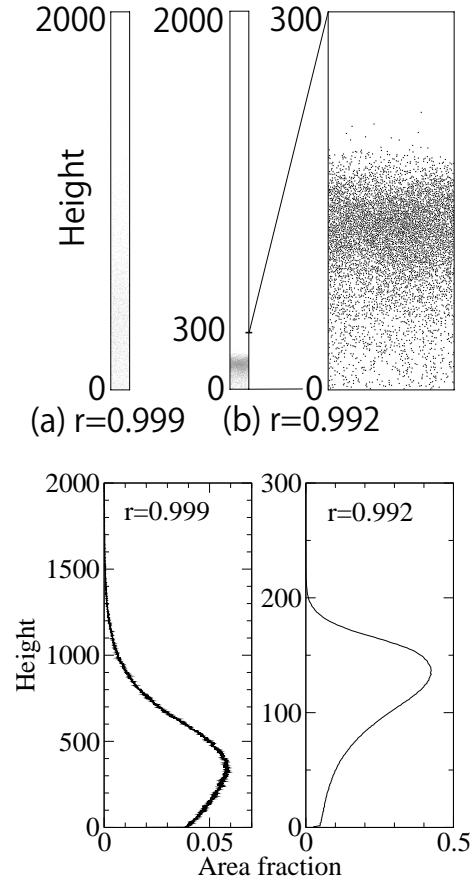


FIG. 1: Top: Snapshots of the two-dimensional simulation with $N = 5000$, $L = 100$ and $g = 10^{-3}$ for different values of restitution coefficient (a) $r = 0.999$; (b) $r = 0.992$. Bottom: Area fraction profiles averaged over a long time period for $r = 0.999$ and $r = 0.992$.

ours [21]. In Ref. [23], it has shown that the density inversion appears above the threshold Λ_c ($\Lambda > \Lambda_c$) where $\Lambda_c \simeq 1.06569$. In the density inversion state, which becomes pronounced for $\Lambda > 2$ as shown in Fig. 1, low density and high temperature gaseous region near the bottom may cause large fluctuations of the dense cluster on top of it. Therefore, this violation of the equipartition of energy should be closely connected to development of density inversion.

Relation between the long time average of the COM height \bar{Z} and the kinetic energy per particle is given in Fig. 3. A linear relation $\bar{Z} = \bar{K}/mg + \text{const.}$ is well satisfied for $\bar{K} > 0.1$ even if the system shows density inversion with a relatively high density cluster. In equilibrium system of dilute gas, the relation $\bar{Z} = \bar{K}/mg + \text{const.}$ holds as a result of statistical mechanics. The fact that \bar{K} characterizes \bar{Z} in the same way as in equilibrium suggests that the global granular temperature T in *inhomogeneous* nonequilibrium state still retains the same meaning as the equilibrium temperature at least in a macroscopic sense.

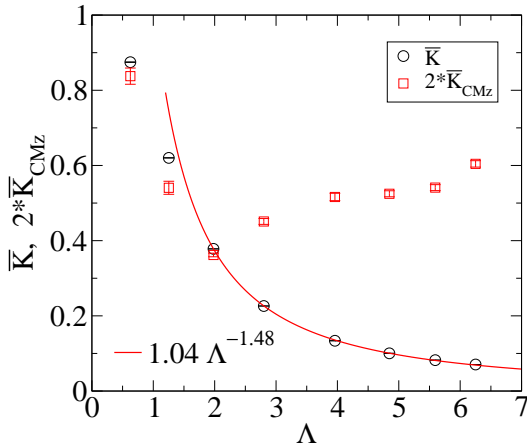


FIG. 2: Kinetic energy per particle \bar{K} (circles) and kinetic energy of the COM \bar{K}_{CMz} (squares) are plotted versus Λ for $r = 0.9999, 0.9996, 0.999, 0.998, 0.996, 0.994, 0.992$, and 0.99 from left to right. The solid line gives a numerical fit of the form $1.04 \times \Lambda^{-1.48}$.

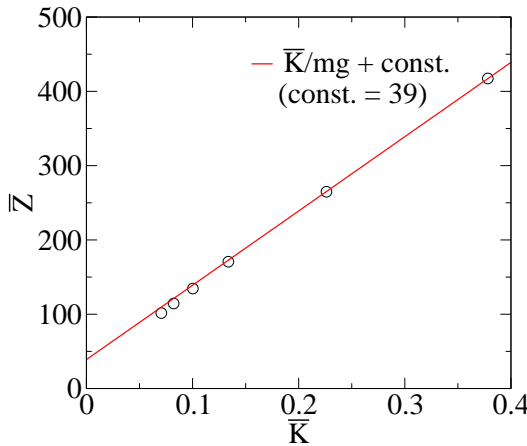


FIG. 3: The average height of the center of mass \bar{Z} versus \bar{K} for $r = 0.9999, 0.9996, 0.999, 0.998, 0.996, 0.994, 0.992$, and 0.99 from right to left. The error bars were smaller than the size of the marks. The solid line gives a linear fit with the slope $(mg)^{-1}$, where $m = 1$ and $g = 10^{-3}$.

In Fig. 4, we plot \bar{K} as a function of the gravitational acceleration g . The dependence of \bar{K} on g turned out to be rather weak. We utilize this fact when we measure response function from simulations in an efficient way (see C in this section).

In Fig. 5, we plotted the probability distribution $P(C)$ of the scaled COM velocity $C \equiv V_z/(2\bar{K}_{CMz}/M)^{1/2}$. The data are fitted sufficiently well by a Gaussian for all cases studied in this paper as is expected from the central limit theorem. This Gaussian property is consistent with our theory based on a linear Langevin equation with an additive Gaussian noise.

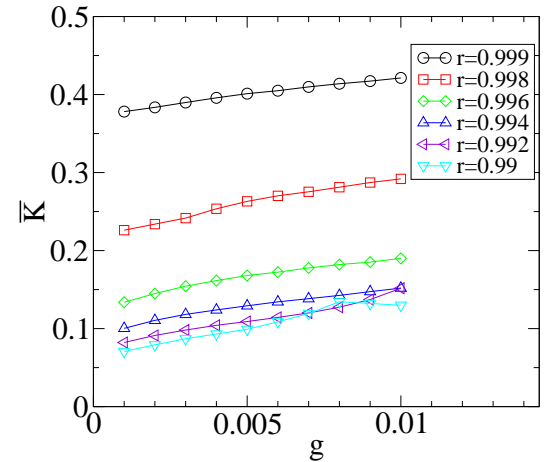


FIG. 4: Kinetic energy per particle \bar{K} is plotted as a function of g . The error bars were smaller than the size of the marks.

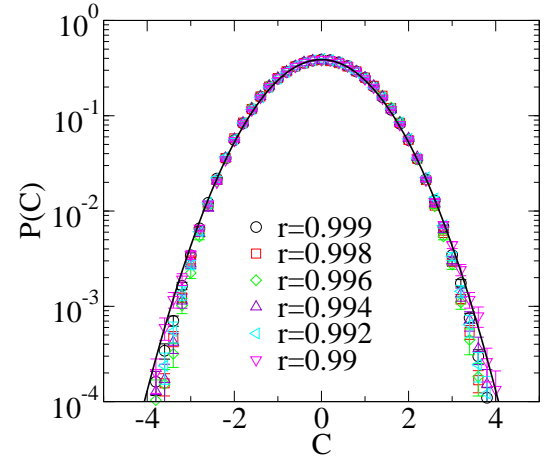


FIG. 5: Probability distribution of the scaled COM velocity $C \equiv V_z/(2\bar{K}_{CMz}/M)^{1/2}$. The solid line is Gaussian with unity dispersion.

B. Power spectrum of the COM height

We first test the theoretical prediction Eq. (8) on the power spectrum of the height of the COM. Using the relation Eq. (6), Eq. (8) can be rewritten as,

$$\begin{aligned} \hat{S}(\hat{\omega}) &\equiv S(\hat{\omega}g/c)/\left[4\left(\frac{c}{g}\right)^3 \frac{\bar{K}_{CMz}}{M}\right] \\ &= \frac{\hat{\mu}}{\left(\hat{\Omega}^2 - \hat{\omega}^2\right)^2 + (\hat{\mu}\hat{\omega})^2}, \end{aligned} \quad (15)$$

where $\hat{\omega}$ is scaled angular frequency defined by $\hat{\omega} \equiv \omega c/g$. This expression suggests that if we scale the power spectrum and the angular frequency as in Eq. (15), it shows a universal behavior independent of any system parameters.

In Fig. 6 (top), we plot the power spectrum $S(\omega)$ for different values of r . The two sharp peaks are observed; one is near zero angular frequency ($\omega = 0$), the other one is at the angular frequency of macroscopic oscillation ($\omega = \omega_{osc}$) which increases as r decreases. The height of both these two peaks decreases as r decreases. We show in Fig. 6 (bottom) the scaled power spectrum $\hat{S}(\hat{\omega})$ that was obtained by scaling $S(\omega)$ in Fig. 6 (top) according to Eq. (15) using c and \bar{K}_{CMz} calculated from simulation data. The theoretical prediction Eq. (8) with fitting numerical parameters $\hat{\mu} = 0.50$, $\hat{\Omega} = 1.7$ is presented as a thick solid line. It is consistent with the results of simulations for a range of $0.99 \leq r \leq 0.994$ in this region near the peak at $\hat{\omega} = \hat{\omega}_{osc} \equiv \omega_{osc}c/g$, in which we expect our theory serves a description to first order approximation. We find large deviations from the theoretical prediction in a region of $\hat{\omega} < \hat{\omega}_{osc}$: the sharp peak near $\hat{\omega} = 0$. As we will illustrate below this peak near $\hat{\omega} = 0$ can be associated with slow fluctuations of global granular temperature due to thermal conduction and collisional dissipation. Since $\tau_{therm}/\tau_{osc} \sim N_z \gg 1$ and $\tau_{diss}/\tau_{osc} \sim [N_z(1-r^2)]^{-1} \geq 1.0$ for our simulations with $N_z = 50$ and $r \geq 0.99$, the contribution of these two processes should appear at $\hat{\omega} < \hat{\omega}_{osc}$. We also find for $r \geq 0.998$, the simulation data in Fig. 6 (bottom) deviate from our theory even in the region near the peak at $\hat{\omega} = \hat{\omega}_{osc}$. These deviations near $\hat{\omega}_{osc}$ might be attributed to the drastic change in density profiles shown in Fig. 1 as r is varied. Concerning our theory, the change in density profiles may affect the numerical coefficients $\hat{\Omega}$ and $\hat{\mu}$ in Eq. (6). Furthermore, in the region $\omega < \omega_{osc}$, the effect of fluctuations of global temperature mentioned above can be pronounced for $r \geq 0.998$ because both τ_{therm} and τ_{diss} become much larger than τ_{osc} , and hence the fluctuations have long life time. We admit that satisfactory explanation of these deviations for $r \geq 0.998$ has not been given yet.

We show here a result of simulations suggesting that behavior of $S(\omega)$ in the region near $\omega = 0$ can be well described by taking into account slow dynamics of $K(t)$. Let us denote the slowly varying part of $K(t)$ as $K'(t)$ and suppose it fluctuates with a much longer time scale than τ_{osc} due to thermal conduction and collisional dissipation. Then, $K'(t)/k_B$ can be regarded as a time-dependent global granular temperature. Similarly, let $Z'(t)$ denote the slowly varying part of $Z(t)$ with the same time scale as $K'(t)$. We assume here that in this long time scale, $K'(t)$ and $Z'(t)$ play the same role as their long time averages \bar{K} and \bar{Z} . That is, they satisfy the same linear relation as their long time averages observed in Fig. 3: $Z'(t) = K'(t)/mg + \text{const.}$ with the same constant factor. If this is the case, the power spectrum of $\delta Z(t)$, $S(\omega)$, in the region near $\omega = 0$ should be given by the power spectrum of $\delta K'(t)/mg$, where $\delta K'(t) = K'(t) - \bar{K}$. In Fig. 7, we show the power spectrum of $\delta K(t)/mg$, where $\delta K(t) = K(t) - \bar{K}$, and $S(\omega)$ for the case of $r = 0.999$ and 0.992 . The figure shows that the curves around the peak in $S(\omega)$ near $\omega = 0$ and

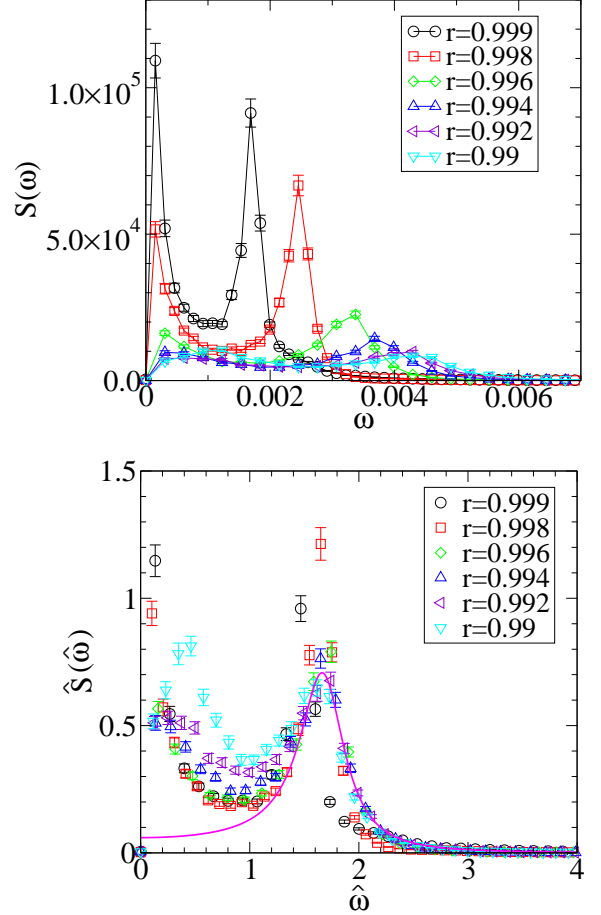


FIG. 6: Top: The power spectrum for the COM height plotted versus angular frequency ω . Bottom: The scaled power spectrum for the COM height. The solid line depicts the theoretical prediction given in Eq. (15) with $\hat{\mu} = 0.50$ and $\hat{\Omega} = 1.7$.

the peak in the power spectrum of $\delta K(t)/mg$ near $\omega = 0$ are consistent. The consistency between the two curves is also observed for the other r values. This result indicates that the peak in $S(\omega)$ near $\omega = 0$ can be accounted for by slow dynamics of $K(t)$ due to thermal conduction and collisional dissipation. It should be stressed that in our present theory fluctuations of granular temperature in both space and time have been ignored and only the global granular temperature T is defined using the long time average of $K(t)$. Further investigation is necessary to construct a theory that fully describes behavior of $S(\omega)$ taking into account the effect of slow fluctuations of granular temperature.

C. Response functions

Next, we test the theoretical prediction Eqs. (11) and (12) on the frequency response functions for the COM. By scaling these functions in the same way as the power

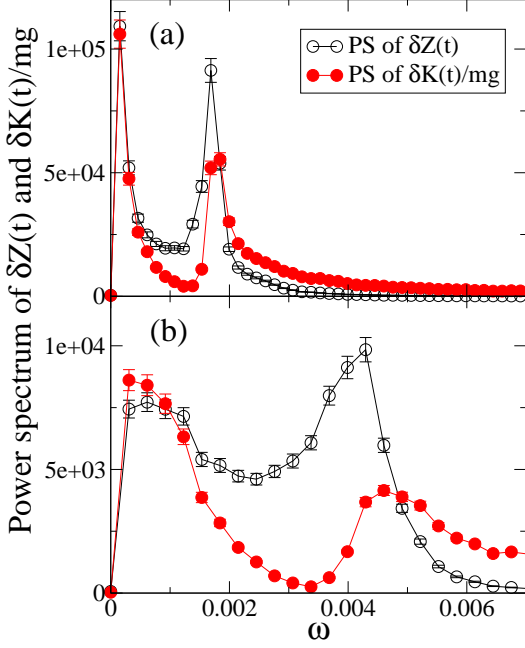


FIG. 7: The power spectrum (PS) of $\delta K(t)/mg$ and the power spectrum of $\delta Z(t)$, $S(\omega)$, for (a) $r = 0.999$ and (b) $r = 0.992$.

spectrum, we can derive universal equations,

$$\hat{\chi}'(\hat{\omega}) \equiv \chi'(\hat{\omega}g/c)Mg^2/c^2 = \frac{\hat{\Omega}^2 - \hat{\omega}^2}{(\hat{\Omega}^2 - \hat{\omega}^2)^2 + (\hat{\mu}\hat{\omega})^2}, \quad (16)$$

$$\hat{\chi}''(\hat{\omega}) \equiv \chi''(\hat{\omega}g/c)Mg^2/c^2 = \frac{\hat{\mu}\hat{\omega}}{(\hat{\Omega}^2 - \hat{\omega}^2)^2 + (\hat{\mu}\hat{\omega})^2}. \quad (17)$$

Measurement of the frequency response function by numerical simulations was performed using the following procedure. First, we prepared for a system in the stationary state with a given N_z , r , and g after sufficiently long time relaxation from the initial state of particles with randomly distributed positions and velocities. At $t = 0$, we exerted a small constant external force to all particles in the direction of gravity and measured the height of the COM at $t > 0$; from this relaxation process of the COM, we can deduce a response function by a standard procedure given in textbooks (see, e.g. Ref. [33]). That is, we measured a response function against a step functional external force. The frequency response function is obtained as the Fourier transform of the response function.

It is important to note that in the response of the COM height against a small but finite external force in our system, *nonlinear* effects resulting from change of time scales are not negligible. This can be seen from the fact that the relevant time scales shown in Eq. (1) all depend on g , and that exerting a constant force in the direction

of gravity is equivalent to changing g . Therefore, a linear response can be defined only in the limit of small external force. This is a point that our Langevin-type theory is different from the well-known Langevin theory for a Brownian motion in a fixed harmonic potential, in which response of Brownian particle is linear against a finite external force. Consequently, we have to exert an external force that is much smaller than the gravitational force in our system in order to measure linear response of the COM height. Because fluctuation of the COM height of the 5000 particles is typically much larger than response against such a small constant force, we need to perform this measurement of the response function for a large number of systems with the same parameters N_z , r , and g but different initial conditions and take an average of the response functions over all realizations. As shown later, in a case of a constant force that is 1% of gravitational force, we needed more than 10^4 realizations to obtain sufficient statistics for getting the clear response functions. This requires relatively long CPU time that impedes carrying out simulations with a wide range of parameters r , N_z and g .

We therefore optimized an efficient method by choosing appropriate parameter to approximately evaluate the response function from small number of realizations, which can be provided by the acceptable time in our computational facilities. Suppose a system with gravitational field g is initially in a NESS and the gravitational acceleration is increased at $t = 0$ from g to $g + \Delta g$. This is equivalent to exert a step functional external force $-M\Delta g\theta(t)$ on the COM height, where $\theta(t)$ is the Heaviside unit step function. Now let us define a function $\chi(t; g, g + \Delta g)$ as

$$\chi(t; g, g + \Delta g) \equiv -\frac{d\langle \delta Z \rangle_t}{dt}/M\Delta g, \quad (18)$$

where $\langle \dots \rangle_t$ represents the average taken over the ensemble of realization δZ at time t . This is a function of Δg in our system due to the nonlinear effects mentioned above; it would equal to the response function only if $\langle \delta Z \rangle_t$ were linear in Δg . Let us denote the Fourier transform of $\chi(t; g, g + \Delta g)$ as $\chi(\omega; g, g + \Delta g)$. According to Eq. (9), the frequency response function $\chi(\omega; g)$ for the system in the stationary state with g is given by

$$\chi(\omega; g) = \lim_{\Delta g \rightarrow 0} \chi(\omega; g, g + \Delta g). \quad (19)$$

We now consider the time scales that we introduced in Sec.IIB, which characterize macroscopic dynamics at $t > 0$. As we discussed in Sec.IIB, all these time scales in the NESS depend on g in the form $\tau = c(g)/g \times \text{const.}$, where we wrote g dependence of c explicitly for the sake of clarity. On the basis of our observation in Fig. 4 that $c(g)$ changes a few percent as g is increased 10%, we assume thermal velocity at $t > 0$ is given by $c(g)$ if Δg is sufficiently small. Thus, these time scales at $t > 0$ have the form $\tau = c(g)/(g + \Delta g) \times \text{const.}$, where $g + \Delta g$ is gravitational acceleration at $t > 0$. This dependence of all the characteristic time scales on Δg leads us to the

following scaling relation:

$$\chi(\omega; g, g + \Delta g) = \frac{1}{M} \left(\frac{c(g)}{g + \Delta g} \right)^2 \hat{\chi} \left(\omega \frac{c(g)}{g + \Delta g} \right), \quad (20)$$

where $\hat{\chi}$ is a nondimensional function.

As far as the scaling relation Eq. (20) holds, we can estimate the limit in Eq. (19) as follows:

$$\chi(\omega; g) = \left(\frac{g + \Delta g}{g} \right)^2 \chi \left(\omega \frac{g + \Delta g}{g}; g, g + \Delta g \right). \quad (21)$$

In order to verify validity of the scaling relation Eq. (20), we carried out two series of simulations for $r = 0.992$: Firstly, we measured the function $\chi(\omega; g, g + \Delta g)$ in Eq. (18) for $\Delta g/g = 10^{-2}$ taking the average over 41000 realizations. Secondly, we measured the frequency response function $\chi(\omega; g)$ using Eq. (21) for $\Delta g/g = 10^{-1}$ taking the average over 800 realizations. In Figs. 8, we compare the frequency response functions obtained from these two series of simulations. We found that they are consistent although there are some discrepancies in $\chi'(\omega)$ near $\omega = 0$.

Another evidence of validity of the scaling relation is the fact that a FDR in an equilibrium system is well satisfied when we measured the frequency response function using Eq. (21), which will be discussed later (see, Fig. 10).

The frequency response functions to be presented below were obtained using the scaling relation Eq. (20) (and Eq. (21)) by averaging over 800 realizations. In Figs. 9, we show the real (top) and imaginary (bottom) parts of the scaled response functions, $\hat{\chi}'$ and $\hat{\chi}''$, as functions of $\hat{\omega}$. Here values of c in Eq. (16) and (17) are calculated in a NESS without perturbation. The theoretical predictions Eqs. (16) and (17) with the same (universal) fitting parameter as estimated in Fig. 6, $\hat{\mu} = 0.50$ and $\hat{\Omega} = 1.7$, are shown by thick lines. It appears that $\hat{\chi}(\omega)$ is consistent with the theoretical predictions if $r \leq 0.996$.

D. Fluctuation-dissipation relation

To test FDR Eq. (13) predicted by our theory, we evaluate the left and right hand sides independently using the results of simulations on $S(\omega)$ (Sec.II.B) and $\chi''(\omega)$ (Sec.II.C) presented in previous subsections. Note that \bar{K}_{CMz} are measured in the NESS where $S(\omega)$ is measured.

At first, we confirmed that the FDR holds within the error bounds of the simulation result in the whole range of ω in the case of $r = 1$ in Fig. 10, in which the stationary state is just the equilibrium state of elastic particles on a thermal wall. In Fig. 11, the left and right hand sides of the FDR are plotted as a function of ω for different r values. For all r ($0.99 \leq r \leq 0.999$), we found that the FDR holds within the error bounds in the range of higher frequency part of ω including a region near the peak $\omega \simeq \omega_p$, which is very close to ω_{osc} defined as the

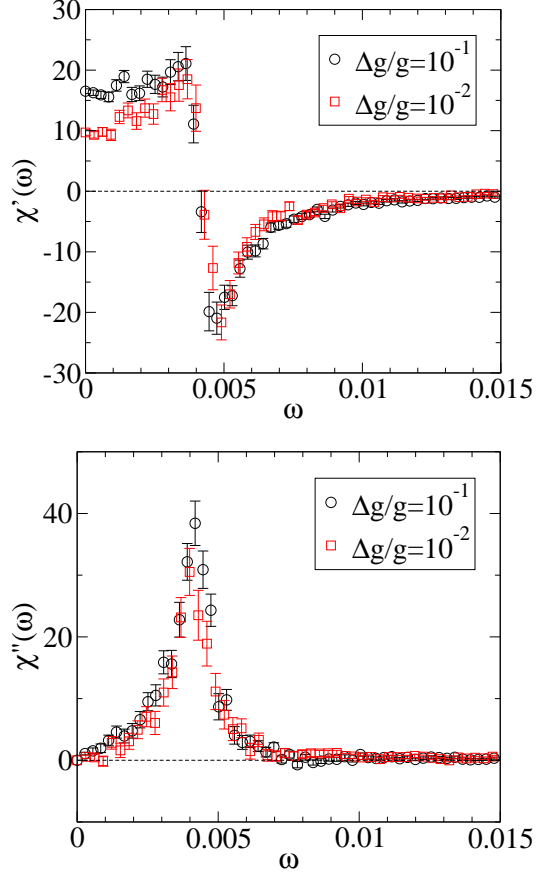


FIG. 8: The real part χ' (top) and the imaginary part χ'' (bottom) of the frequency response function plotted versus angular frequency ω for $r = 0.992$. Circles are the data for $\Delta g/g = 10^{-2}$ without using Eq. (21); averages have been obtained over 41000 realizations. Squares are for $\Delta g/g = 10^{-1}$ using Eq. (21) with averages obtained over 800 realizations.

angular frequency of a peak in $S(\omega)$. We stress here that we defined T_{eff} as $T_{eff} = 2\bar{K}_{CMz}/k_B$ in the FDR. The quantitative agreement in Fig. 11 supports this definition of T_{eff} using \bar{K}_{CMz} instead of using the global granular temperature T since T_{eff} is more than three times as large as T for $r \leq 0.996$ (see Fig. 2).

We found systematic deviations in a region $\omega < \omega_p$. These deviations are attributed to an existence of a peak near $\omega = 0$ in $S(\omega)$ shown in Fig. 6. As we have discussed in Sec.IV B, the peak near $\omega = 0$ could be connected with slow fluctuations of granular temperature due to thermal conduction and collisional dissipation. For $r = 0.999$, time scales of these two processes, τ_{therm} and τ_{diss} become much larger than τ_{osc} , and thus the fluctuations with long life time might be responsible for the deviation at small ω . For $r \leq 0.994$, the deviation seems to increase as r decreases. Since the system has less granular temperature for smaller r , larger heat current from the thermal wall is induced, and it could cause larger fluctuations in global granular temperature. Further in-

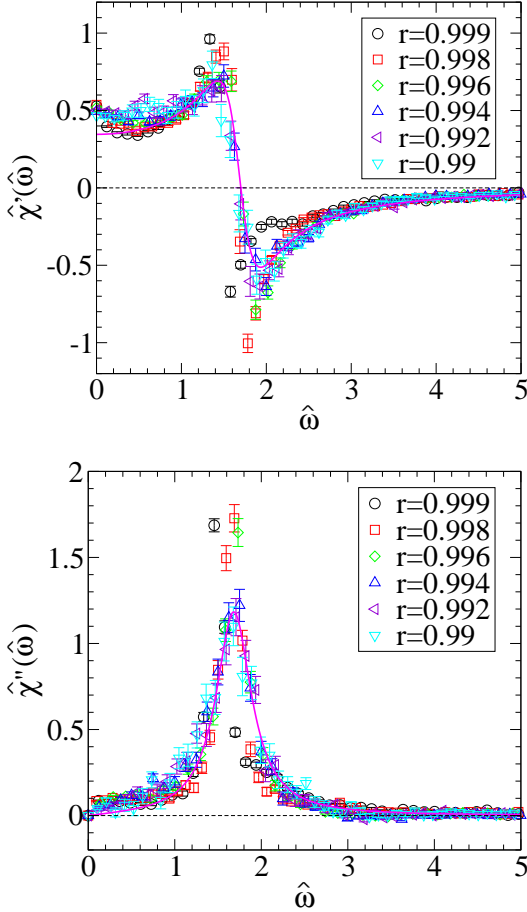


FIG. 9: The real (top) and imaginary part (bottom) of the scaled frequency response function plotted versus scaled angular frequency $\hat{\omega} = \omega c/g$. Averages have been taken over 800 realizations. The thick lines are the theoretical prediction Eqs. (16) and (17) with fitting parameters: $\hat{\mu} = 0.50$, $\hat{\Omega} = 1.7$.

vestigation is necessary to understand more precisely this violation of the FDR.

V. CONCLUSION

In this paper we have studied validity of the fluctuation-dissipation relation with regard to the COM motion in a NESS of a driven granular fluid under gravity. By neglecting fluctuations of global temperature caused by thermal conduction and collisional dissipation, which change much slower than macroscopic oscillation of the fluid, we have derived a Langevin equation for the COM height. This Langevin equation predicts functional forms of the correlation and response functions for the COM height that contain two phenomenological numerical constants $\hat{\mu}$ and $\hat{\Omega}$ to be used as fitting parameters. It also gives a fluctuation-dissipation relation accompanied with an effective temperature T_{eff} that characterizes agit-

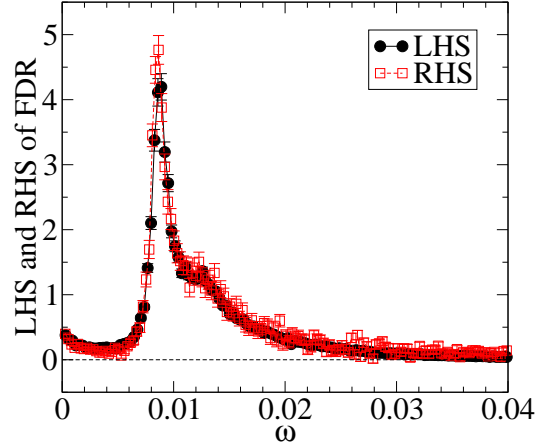


FIG. 10: The left hand side $\omega S(\omega)/2k_B T_{eff}$ and the right hand side $\chi''(\omega)$ of Eq. (13) for $r = 1$. $N = 5000$, $L = 100$ and $g = 10^{-2}$ with averages over 400 realizations for $S(\omega)$ and over 800 realizations for $\chi''(\omega)$.

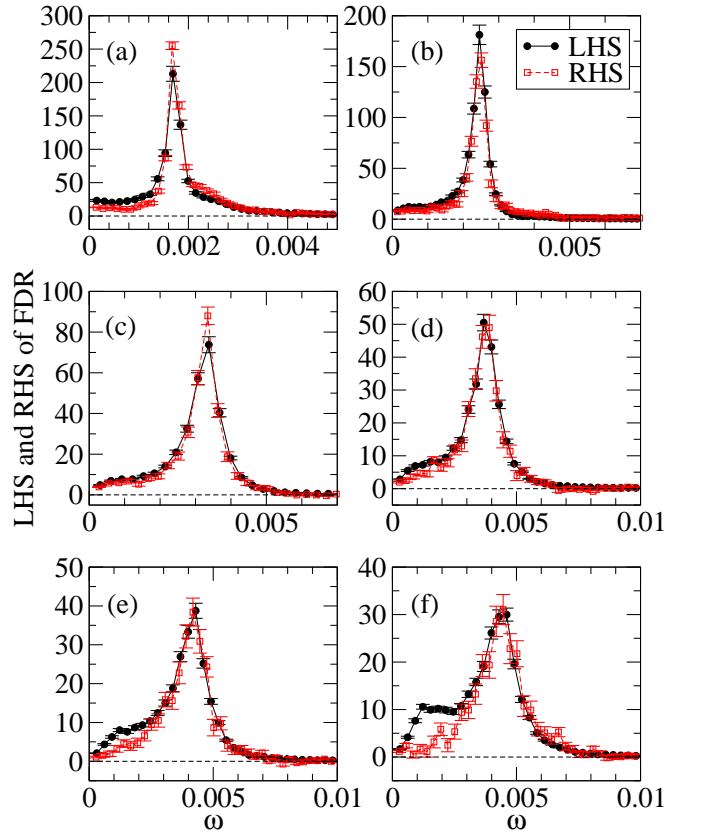


FIG. 11: The left hand side $\omega S(\omega)/2k_B T_{eff}$ and the right hand side $\chi''(\omega)$ of Eq. (13) for (a) $r = 0.999$, (b) $r = 0.998$, (c) $r = 0.996$, (d) $r = 0.994$, (e) $r = 0.992$, and (f) $r = 0.99$. $N = 5000$, $L = 100$ and $g = 10^{-3}$ with averages over 400 realizations for $S(\omega)$ and over 800 realizations for $\chi''(\omega)$.

ing motion of the COM height by $T_{eff} = 2\bar{K}_{CMz}/k_B$.

In order to test the fluctuation-dissipation relation, we have performed event-driven MD simulations and measured the power spectrum and response function for the COM height. While the power spectrum was consistent with our theory for $r \leq 0.994$ and ω around the angular frequency of the slowest oscillation of the COM, it also showed large deviations from the theoretical prediction near $\omega = 0$ and deviations for $r > 0.994$. The response function agreed well with our theory for $r \leq 0.996$ but showed deviations for $r > 0.996$. Furthermore, we compared the left and right hand sides of the fluctuation-dissipation relation. The results showed that they were consistent in a region of ω near the largest peak, but deviations occurred near $\omega = 0$. These deviations are originated from the power spectrum for the COM height, showing a sharp peak near $\omega = 0$, which cannot be described by our theory.

We showed that these deviations near $\omega = 0$ can be attributed to slow fluctuations of global temperature defined as slowly varying part of kinetic energy per particle $K(t)$ due to thermal conduction and collisional dissipation; these fluctuations of global temperature have been neglected in our theory. The deviations in the power spectrum and resulting violation of the FDR are expected to be accounted for by a theory that describes both of $Z(t)$ and $K(t)$, which will be investigated in our future study.

In Ref. [34] a formula that connects violation of the FDR in a NESS with the energy dissipation or equivalently energy input from outside has been proposed. A theory extended to include slow dynamics of $K(t)$ and direct measurement of energy input in our simulations might give some insight to generality of their formula.

Finally, we mention that a basic question whether the effective temperature T_{eff} obtained here has any physical meaning as temperature in thermodynamics is still unclear. Definition of effective temperature in a system that relaxes in several time scales, typically glass, have been argued in Ref. [2, 35]. It would be interesting to apply their theory to our problem with three time scales τ_{therm} , τ_{diss} and τ_{osc} . It would become also important to investigate via extensive simulation what happens if two systems with different effective temperature are in contact with each other. These studies would measure the direction of heat flow directly which might clarify an insight and physical meaning of the effective temperature.

Acknowledgments

J. W. is grateful to H. Nakanishi, T. Sakaue, T. Saito, and C. Nakajima for their hospitality during his stay at Kyushu university where part of this study was done. This study was supported by Grant-in-Aid for Scientific Research from the Ministry of Education, Culture, Sports, Science and Technology No. 23740293. Part of the computations for this study was performed us-

ing the facilities of the Supercomputer Center, Institute for Solid State Physics, the University of Tokyo, and Research Center for Computational Science(RCCS), Okazaki, Japan.

Appendix A: Langevin equation

In this section, we summarize derivation [20, 21] of the Langevin equation that describes the motion of the COM of grains.

The equation of motion for the COM of grains in the model described in Sec.II can be written in the following form:

$$M \frac{d^2 Z}{dt^2} = -Mg + F_b. \quad (A1)$$

The right hand side of the equation of motion for the COM must be, in general, the sum of the external forces acting on the grains. In our model, they are the gravitational force $-Mg$ and the z -component of the force exerted by the bottom wall F_b . Thus, it is essential to understand property of F_b for the study of COM motion.

Let us consider its reaction force $F'_b (= -F_b)$, the force exerted by grains against the bottom wall. A snapshot of the granular fluid is sketched in Fig. 12 (a). Suppose the COM is at a height Z and is moving downward, for instance, with a velocity V . Let us now change the frame of reference to the center of mass frame (see Fig. 12 (b)). It looks then the bottom wall that lies the distance Z away from the COM in the z -direction, is moving upward with the velocity $-V$. Now the problem is how to determine F'_b , the force acting on the bottom wall as a result of frequent collisions of granular particles, in the situation shown in Fig. 12 (b), in which the bottom wall is moving upward with the velocity $-V$ against the macroscopically static fluid.

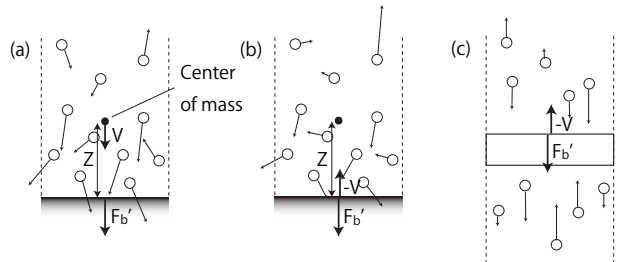


FIG. 12: (a) a sketch of the system observed in the laboratory frame of reference, (b) the same system observed in the center of mass frame, (c) the Rayleigh piston: a piston undergoes random collisions with a one-dimensional heat bath of particles.

This problem is similar to the problem of determining the force acting on a one-dimensional Brownian particle, which is referred to as the Rayleigh piston [19], moving in the z -directions with a velocity $-V$ (see Fig. 12 (c)).

We model an expression of F'_b on the basis of this analogy with Brownian motion, and assume that F'_b consists of the following three components: The first is a systematic force $f_P(t)$ which equals to the pressure multiplied by the area of the bottom wall. Since local density near the bottom wall changes according to the motion of the COM, this force may depend on time. Apparently the long time average of $f_P(t)$, say $\overline{f_P}$, must be equal to Mg , the gravitational force acting on all particles. The simplest assumption on the time dependent part of $f_P(t)$ is that it is proportional to deviation of the COM height from its stationary value, $Z(t) - \overline{Z}$, since change in the local density near the bottom wall could be proportional to $-(Z(t) - \overline{Z})$ if the change in the height of the COM is sufficiently small: $|Z(t) - \overline{Z}|/\overline{Z} \ll 1$. The second is a frictional force. We assume here the simplest form of the frictional force that is linear in the relative velocity $-V(t)$ of the bottom wall to the COM. The third is a random force. Thus, we assume the following form:

$$\begin{aligned} F'_b(t) &= -Mg + M\Omega^2(Z(t) - \overline{Z}) + M\mu V(t) + R'(t) \\ &= -F_b(t), \end{aligned} \quad (\text{A2})$$

where Ω is a coefficient that specifies the angular frequency of the slowest oscillation of the COM, and μ is the frictional coefficient. According to the discussion on the characteristic time scales in Sec.IIB, the time scales for macroscopic oscillation τ_{osc} and that for pressure relaxation τ_p are $\tau_{osc} \sim \tau_p \sim c/g$. Thus, we assume

$$\Omega = \hat{\Omega}/\tau_{osc} = \hat{\Omega}g/c, \quad \mu = \hat{\mu}/\tau_p = \hat{\mu}g/c. \quad (\text{A3})$$

As property of the random force, we assume stationary Gaussian white noise in the same way as the Rayleigh piston:

$$\langle R'(t) \rangle = 0, \quad \langle R'(t)R'(t') \rangle = I\delta(t - t'). \quad (\text{A4})$$

where I represents the intensity of the random force.

Substituting F_b obtained in (A2) into the equation of motion of the COM (A1), we obtain

$$\frac{d^2\delta Z}{dt^2} = -\Omega^2\delta Z - \mu\frac{d\delta Z}{dt} + \frac{R(t)}{M}, \quad (\text{A5})$$

where $\delta Z \equiv Z(t) - \overline{Z}$ and $R(t) = -R'(t)$. The random force $R(t)$ has the exactly same property described in (A4) as $R'(t)$. Note that the Langevin equation (A5) has the same form as that describes Brownian motion in a harmonic potential.

Appendix B: Derivation of the power spectrum and the response function

Since derivation of the power spectrum and the response function from the Langevin equation describing Brownian motion in a harmonic potential is given in textbooks (see, e.g., Ref. [36]), we present here only essential steps in their calculation. Let us first consider the power spectrum of the fluctuating motion of the COM obeying the Langevin equation (A5). The formal solution of

Eq. (A5) is written as

$$Z(t) - \overline{Z} = \int_{-\infty}^t G(t - t') \frac{R(t')}{M} dt' + F_{ini}(t), \quad (\text{B1})$$

where the function $G(t)$ is given by

$$G(t) = \frac{e^{-\frac{\mu}{2}t}}{\omega_0} \sin(\omega_0 t), \quad (\text{B2})$$

and ω_0 is defined by $\omega_0 \equiv (\Omega^2 - (\mu/2)^2)^{1/2}$. The last term $F_{ini}(t)$ in Eq. (B1) consists of those that depend on the initial conditions and vanish after a sufficient amount of time. Thus, the term is negligible when calculating long-time averages of physical quantities in the stationary state.

Using this formal solution, one can calculate the two-time correlation function $\phi(t)$ in a NESS defined by $\phi(t) \equiv \lim_{t' \rightarrow \infty} \langle \delta Z(t')\delta Z(t' + t) \rangle$, where the brackets $\langle \dots \rangle$ indicate an average over the random force $R(t)$. We took the limit $t' \rightarrow \infty$ in order to assure the system to be in the stationary state.

The power spectrum of $\delta Z(t)$ can be obtained using the Wigner-Khinchin theorem:

$$S(\omega) = \int_{-\infty}^{\infty} dt e^{-i\omega t} \phi(t) \quad (\text{B3})$$

$$= \frac{I}{M^2} \frac{1}{(\Omega^2 - \omega^2)^2 + (\mu\omega)^2}. \quad (\text{B4})$$

Next, let us consider the response function for the COM, which describes linear response of the COM with regard to a small external force $\varepsilon f(t)$. The Langevin equation in this case is written as

$$\frac{d^2\delta Z}{dt^2} + \Omega^2\delta Z + \mu\frac{d\delta Z}{dt} - \frac{\varepsilon f(t)}{M} - \frac{R(t)}{M} = 0. \quad (\text{B5})$$

Taking the average over the random force, we obtain

$$\frac{d^2\langle \delta Z \rangle}{dt^2} + \Omega^2 \langle \delta Z \rangle + \mu \frac{d\langle \delta Z \rangle}{dt} - \frac{\varepsilon f(t)}{M} = 0. \quad (\text{B6})$$

The response function $\chi(t)$ is defined as

$$\langle \delta Z(t) \rangle = \int_{-\infty}^t dt' \chi(t - t') \varepsilon f(t'). \quad (\text{B7})$$

Here the external force $\varepsilon f(t)$ is assumed to be infinitely small. The Fourier transform of this relation yields $\langle \delta \tilde{Z}(\omega) \rangle = \chi(\omega) \varepsilon \tilde{f}(\omega)$, and hence

$$\chi(\omega) = \lim_{\varepsilon \rightarrow 0} \langle \delta \tilde{Z}(\omega) \rangle / \varepsilon \tilde{f}(\omega). \quad (\text{B8})$$

Performing the Fourier transform of the relation (B6) and comparing it with Eq. (B8), we obtain the frequency response function (complex admittance)

$$\chi(\omega) = \frac{1}{M} \frac{1}{\Omega^2 - \omega^2 + i\mu\omega}. \quad (\text{B9})$$

-
- [1] I. S. Aranson and L. S. Tsimring, *Rev. Mod. Phys.* **78**, 641 (2006).
- [2] L. F. Cugliandolo, *J. Phys. A: Math. Theor.* **44**, 483001 (2011).
- [3] U. M. B. Marconi, A. Puglisi, L. Rondoni, and A. Vulpiani, *Phys. Rep.* **461**, 111 (2008).
- [4] I. Goldhirsch and T. P. C. van Noije, *Phys. Rev. E* **61**, 3241 (2000).
- [5] J. W. Dufty and V. Garzó, *J. Stat. Phys.* **105**, 723 (2001).
- [6] J. W. Dufty and J. J. Brey, *J. Stat. Phys.* **109**, 433 (2002).
- [7] J. Dufty, A. Baskaran, and J. J. Brey, *J. Stat. Mech. Theory Exp.* L08002 (2006).
- [8] J. Duran, *Sands, Powders, and Grains: An Introduction to the Physics of Granular Materials* (Springer Verlag, New York, 2000).
- [9] A. Puglisi, A. Baldassarri, and V. Loreto, *Phys. Rev. E* **66**, 061305 (2002).
- [10] V. Garzó, *Physica A* **343**, 105 (2004).
- [11] A. Puglisi, A. Baldassarri, and A. Vulpiani, *J. Stat. Mech. Theory Exp.* P08016 (2007).
- [12] G. Bunin, Y. Shokef, and D. Levine, *Phys. Rev. E* **77**, 051301 (2008).
- [13] J. J. Brey and M. J. Ruiz-Montero, *Phys. Rev. E* **81**, 021304 (2010).
- [14] H. A. Makse and J. Kurchan, *Nature* **415**, 614 (2002).
- [15] A. Barrat, V. Colizza, and V. Loreto, *Phys. Rev. E* **66**, 011310 (2002).
- [16] C. S. O'Hern, A. J. Liu, and S. R. Nagel, *Phys. Rev. Lett.* **93**, 165702 (2004).
- [17] G. D'Anna, P. Mayor, A. Barrat, V. Loreto, and F. Nori, *Nature* **424**, 909 (2003).
- [18] S. Warr, J. M. Huntley, and G. T. H. Jacques, *Phys. Rev. E* **52**, 5583 (1995).
- [19] N. G. van Kampen, *Stochastic Processes in Physics and Chemistry*, (Elsevier Science, Amsterdam, 1992).
- [20] J. Wakou, A. Ochiai, and M. Isobe, *J. Phys. Soc. Jpn.*, **77**, 034402 (2008).
- [21] J. Wakou and M. Isobe, in *Proceedings in Joint IUTAM-ISIMM Symposium on Mathematical Modeling and Physical Instances of Granular Flows, 2009*: AIP Conf. Proc. (USA), **1227**, 135 (2010).
- [22] J. J. Brey, M. J. Ruiz-Montero, and F. Moreno, *Phys. Rev. E* **63**, 061305 (2001).
- [23] Y. Bromberg, E. Livne, and B. Meerson, in *Granular Gas Dynamics*, edited by T. Pöschel and N. Brilliantov (Springer-Verlag, Berlin, 2003), pp. 251-266.
- [24] L. D. Landau and E. M. Lifshitz, *Fluid mechanics* (Pergamon Press, New York, 1987).
- [25] S. Chapman and T. G. Cowling, *The Mathematical Theory of Non-Uniform Gases*, (Cambridge University Press, Cambridge, 1970).
- [26] S. Luding, E. Clément, A. Blumen, J. Rajchenbach, and J. Duran, *Phys. Rev. E*, **49**, 1634 (1994).
- [27] H.-Q. Wang and N. Menon, *Phys. Rev. Lett.* **100**, 158001 (2008).
- [28] M. Isobe, *Int. J. Mod. Phys.*, **C10**, 1281 (1999).
- [29] A. Kudrolli, M. Wolpert, and J. P. Gollub, *Phys. Rev. Lett.* **78**, 1383 (1997).
- [30] R. D. Wildman, J. M. Huntley, and J.-P. Hansen, in *Granular Gases*, edited by T. Pöschel and S. Luding (Springer-Verlag, Berlin, 2001), pp. 215-232.
- [31] Y. Lan and A. D. Rosato, *Phys. Fluids* **7**, 1818 (1995).
- [32] M. Isobe, and H. Nakanishi, *J. Phys. Soc. Jpn.*, **68**, 2882 (1999).
- [33] R. Kubo, M. Toda, and N. Hashitsume, *Statistical Physics II*, (Springer-Verlag, Berlin, 1991).
- [34] T. Harada and S.-I Sasa, *Phys. Rev. Lett.* **95**, 130602 (2005).
- [35] L. F. Cugliandolo, J. Kurchan, and L. Peliti, *Phys. Rev. E* **55**, 3898, (1997).
- [36] P. Résibois and M. De Leener, *Classical Kinetic Theory of Fluids*, (Jhon Wiley & Sons Inc, New York, 1977).